

ACID–BASE PROPERTIES OF A CERIA–LANTHANA CATALYTIC SYSTEM

An adsorption microcalorimetry study

M. G. Cutrufello^{1*}, *I. Ferino*¹, *E. Rombi*¹, *V. Solinas*¹, *G. Colón*²
and *J. A. Navío*²

¹Dipartimento di Scienze Chimiche, Università di Cagliari, Complesso Universitario di Monserrato, s.s. 554 bivio per Sestu, 09042 Monserrato (Ca), Italy

²Instituto de Ciencia de Materiales, Centro de Investigaciones Científicas ‘Isla de la Cartuja’, Centro Mixto CSIC-Universidad de Sevilla, Avda. Américo Vespucio s/n, 41092 Sevilla, Spain

Abstract

A ceria–lanthana system was prepared by the sol–gel technique in order to obtain active catalysts for the 4-methylpentan-2-ol conversion. As the products distribution strongly depends on the acid–base features of the catalyst, acidity and basicity of the CeO₂–La₂O₃ samples were determined by adsorption microcalorimetry, using ammonia and carbon dioxide as probe molecules. Both concentration and strength of the sites were assessed and their nature was investigated by analysing the microcalorimetric data in the light of the structural and textural characterisation previously carried out. Present samples are compared to a formerly investigated ceria–lanthana system prepared by a different procedure.

Keywords: acidity, basicity, ceria, lanthana, microcalorimetry

Introduction

Adsorption microcalorimetry is known to be one of the most reliable methods for studying the surface acidity and basicity of solid catalysts [1]. By the simultaneous assessment of the adsorbed amount of a suitable probe molecule and the heat evolved at increasing coverage, both the quantitative and the energetic features of the surface sites can be described.

Among the reactions catalysed by the acid–base sites of solids, secondary alcohols dehydration has been widely investigated. The dehydration of 4-methylpentane-2-ol could represent a convenient way for producing 4-methylpent-1-ene, starting material for the manufacture of polymers of superior technological properties. The fine tuning of the acid–base features of the catalyst surface has proved to be essential in governing the competition between the dehydration and the parasitic dehydrogenation of the reactant alcohol, as well as the formation of the desired 4-methylpent-1-ene among the dehydration products [2–8].

* Author for correspondence: E-mail: gcutrufe@unica.it

In two previous papers [9, 10] a ceria-lanthana catalytic system prepared by the sol-gel technique from nitrate precursors was widely investigated. The present paper deals with a CeO₂-La₂O₃ catalytic system prepared by a variant of the above-mentioned method, involving the addition of hydrogen peroxide before the precipitation. The structural and morphological characterisation of the samples obtained through this procedure has already been presented in detail [9]. Here their acid-base features, investigated by means of adsorption microcalorimetry using ammonia and carbon dioxide as probe molecules, are reported.

Experimental

Cerium-lanthanum mixed oxides were prepared by means of a sol-gel method from nitrate precursors, Ce(NO₃)₃·6H₂O and La(NO₃)₃·6H₂O. Corresponding amounts of each rare-earth nitrate solution were mixed and hydrogen peroxide was then added in a molar ratio of 10:1. A gel was obtained by raising the pH up to 9 by the addition of aqueous ammonia. After a 30 min ageing under stirring, the gel was filtered, washed several times with distilled water and dried at 383 K overnight. Five samples of different compositions were then obtained by calcining the fresh powders at 873 K for 2 h.

The samples will hereafter be referred to as C_xLa(100-*x*)H, where *x* is the nominal (and bulk) cerium atomic percentage and H indicates the use of hydrogen peroxide during the preparation, in order to distinguish the present samples from those previously studied, referred to as C_xLa(100-*x*) [9, 10]. The bulk and surface composition of the samples, as well as their structural and textural features, are summarised in Table 1. Further details are reported elsewhere [9].

Table 1 Characteristics of the catalysts^a

Sample	Chemical composition/Ce atom%		Crystal phase	Surface area/ m ² g ⁻¹
	Bulk	Surface		
Ce100H	100	100	cubic CeO ₂	48.5
Ce75La25H	75	83	cubic mixed oxide	52.6
Ce50La50H	50	58	cubic mixed oxide	40.0
Ce25La75H	25	54	cubic mixed oxide	40.5
La100H	0	0	hexagonal La ₂ O ₃ hexagonal La(OH) ₃	20.5

^aData from [9]

Microcalorimetric measurements were carried out in a Tian-Calvet heat flow equipment (Setaram). Each sample was pretreated overnight at 673 K under vacuum (10⁻³ Pa) before the successive introduction of small doses of the probe gas (ammonia or carbon dioxide). The equilibrium pressure relative to each adsorbed amount was measured by means of a differential pressure gauge (Datametrics). The run was

stopped at a final equilibrium pressure of 133.3 Pa. The adsorption temperature was maintained at 353 K, in order to limit physisorption. The adsorption and calorimetric isotherms were obtained from each adsorption experiment. They relate, respectively, the amount of probe gas and the integral heat of adsorption with the corresponding equilibrium pressure. Combining the two sets of data, a plot of the differential heat of adsorption, Q_{diff} , as a function of the adsorbed amount was drawn, which gives information on the influence of surface coverage on the energetics of the adsorption.

Results

The microcalorimetric results for all the samples are summarised in Fig. 1, where the differential heats, Q_{diff} , for both NH_3 and CO_2 adsorption are plotted vs. uptake.

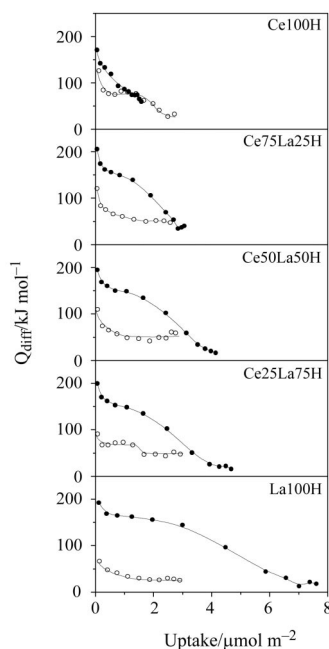


Fig. 1 Differential heat of adsorption, Q_{diff} , vs. uptake of \circ – ammonia and \bullet – carbon dioxide

The initial Q_{diff} value for the NH_3 adsorption changes regularly within the series of catalysts, being the highest for Ce100H (126 kJ mol^{-1}) and the lowest for La100H (66 kJ mol^{-1}). Whatever the sample, the adsorption heat decreases with increasing ammonia uptake, until the total coverage is reached (ca. $3 \mu\text{mol m}^{-2}$ for any catalyst). The Q_{diff} profile for Ce100H forms a step at ca. 80 kJ mol^{-1} , before gently decreasing to lower values (around 30 kJ mol^{-1}). The curves for Ce75La25H, Ce50La50H and La100H gradually decrease from the initial to a practically constant Q_{diff} value (respectively 50 , 51 and 28 kJ mol^{-1}). The Q_{diff} curve for Ce25La75H shows a peculiar pattern, with two distinct steps (at 70 and 48 kJ mol^{-1}).

The initial Q_{diff} values for the CO_2 adsorption are all around 200 kJ mol^{-1} . Only Ce100H possesses a lower initial adsorption heat (171 kJ mol^{-1}), which gradually decreases with coverage. No CO_2 adsorption occurs at Q_{diff} values below 60 kJ mol^{-1} for this catalyst. The Q_{diff} profiles for all the other samples show, after the first points, a step (at ca. 150 kJ mol^{-1} for the mixed samples, at slightly higher values – around 160 kJ mol^{-1} – for La100H), whose extent increases with the lanthanum content. Also the total amount of adsorbed CO_2 increases noticeably along the series of catalysts, reaching $7.6 \mu\text{mol m}^{-2}$ for La100H. Moreover, the four La-containing samples also show a set of points characterised by a low heat of adsorption (ca. 37 kJ mol^{-1} for Ce75La25H; $15\text{--}25 \text{ kJ mol}^{-1}$ for the others), which is clearly related to the presence of La, as it is absent in Ce100H.

Discussion

The microcalorimetric curves (Fig. 1) provide information about the acid–base features of the samples, in terms of number and strength of the sites. Ammonia adsorption indicates that the strength of the acid sites slightly decreases along the series (from Ce100H to La100H), although their total concentration is quite constant. The presence of a set of homogeneous sites is shown by all the catalysts, with the exception of Ce25La75H, whose acid sites form two different families. In the $\text{Ce}_x\text{La}_{(100-x)}$ series [9] the heat of adsorption fell to lower values (well below 35 kJ mol^{-1}); such a weak interaction was ascribed to physical adsorption and thus disregarded when estimating the number of acid sites. For the present samples, only the last points for Ce100H and part of the La100H curve are below 40 kJ mol^{-1} , while the mixed samples do not present such weak sites, even at high coverage.

The surface species responsible for acidity in metal oxides are coordinatively unsaturated (c.u.s.) metal ions. Hence in the present samples the acid sites are c.u.s. Ce^{4+} and La^{3+} ions. On average, the adsorption heat of ammonia decreases while the La content increases, indicating a lower acid strength of the La^{3+} sites, in comparison with the Ce^{4+} , which is in agreement with the charge/radius value, lower for La^{3+} than for Ce^{4+} . The presence of two sets of acid sites is observed in the Ce25La75H sample; they can reasonably be associated with two different phases: (i), a $\text{CeO}_2\text{--La}_2\text{O}_3$ solid solution of composition not too different from the nominal one, with Q_{diff} ca. 48 kJ mol^{-1} , like the acid sites observed in Ce75La25H and Ce50La50H; (ii), a segregated ceria-rich phase (or even a pure ceria phase), with Q_{diff} ca. 70 kJ mol^{-1} , similar to the acid sites on the Ce100H sample. The segregation of such a ceria-rich phase on the surface of Ce25La75H is also suggested by the considerable difference between the Ce percentage in the bulk and on the surface for this sample (Table 1).

The Q_{diff} vs. CO_2 uptake profiles for Ce100H and La100H (Fig. 1) reveal noticeable differences between the two ‘single-metal’ catalysts. Ce100H clearly shows a heterogeneous strength distribution of the basic sites, which can be identified with c.u.s. oxygen ions bonded to Ce. Instead, La100H presents two sets of sites: a strong one (160 kJ mol^{-1}), responsible for the wide step, and a weak one, responsible for the final part of the curve. The former is reasonably originated by the oxygen ions

bonded to La in the oxide; the latter is probably due to weakly basic OH groups of superficial hydroxycarbonate-like species, whose presence was revealed by FTIR analysis [9]. The two families typical of La100H are also observed for the mixed ceria-lanthana samples, being more and more populated as the lanthanum content increases. The introduction of La into the ceria lattice had the same effect on the basic sites distribution (i.e. the appearance of the two families, revealed in the CO₂ adsorption curves by the presence of the points at low Q_{diff} and of the step at high adsorption heat values, whose extent increases with the La content) in the case of the ceria-lanthana samples prepared without H₂O₂ [10]. However, an important difference between the present samples and the CexLa(100-x) series can be evidenced. La100 was characterised by very high initial Q_{diff} values (390 kJ mol⁻¹), which fell to very low values (<15 kJ mol⁻¹) at high coverage. No step could be seen in the curve. According to XRD results, La100 was found to be constituted only by La(OH)₃, whose OH groups were assumed to be the strong sites revealed by the microcalorimetric experiments. The XRD data for La100H showed that the present sample is mostly constituted by La₂O₃, with a minor contribution of La(OH)₃; correspondingly, no sites with $Q_{\text{diff}} > 200$ kJ mol⁻¹ are revealed by CO₂ adsorption (Fig. 1).

From Fig. 1 data, the total concentration of acid and base sites (n_A and n_B respectively) have been obtained; the points with $Q_{\text{diff}} < 25$ kJ mol⁻¹ have been disregarded in the calculation, as the corresponding sites are too weak to be considered active at the operating conditions of the catalytic reaction in which the samples are to be tested.

In Fig. 2, n_A and n_B are plotted vs. the surface composition. It can be noted that while n_A is practically the same for all the catalysts, n_B increases regularly with the lanthanum content. Such a linear trend was not followed by the CexLa(100-x) series [10], for which n_A slightly decreased and n_B showed a maximum as the La-content increased. Actually, the most important difference between the two series is shown by La100 ($n_A = 1.4$ μmol m⁻², $n_B = 2.8$ μmol m⁻²) and La100H ($n_A = 2.9$ μmol m⁻², $n_B = 6.7$ μmol m⁻²). As already mentioned, the same two samples also show a different strength distribution of the basic sites. Although they both are basic catalysts, the nature of their basicity is different: La100 showed very strong basic sites, while La100H is characterised by a high concentration of basic sites.

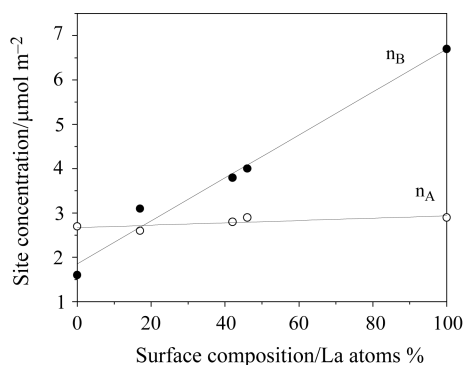


Fig. 2 Influence of the surface composition on the o – acid-site and ● – base-site concentrations

Table 2 Basic sites concentration to acid sites concentration ratio (n_B/n_A) and fraction of acid ($n_{A\geq 70}/n_A$) and basic sites ($n_{B\geq 70}/n_B$) with $Q_{\text{diff}}\geq 70$ kJ mol⁻¹

Sample	n_B/n_A	$n_{A\geq 70}/n_A$	$n_{B\geq 70}/n_B$
Ce100H	0.6	0.56	0.92
Ce75La25H	1.2	0.18	0.78
Ce50La50H	1.4	0.12	0.77
Ce25La75H	1.4	0.44	0.75
La100H	2.3	0.00	0.77

Analysing the results obtained for the catalytic systems previously investigated, a rationale for interpreting the catalytic behaviour in the 4-methylpentan-2-ol conversion on the basis of the microcalorimetric data has been formulated, which takes into account both the concentration and the strength of the sites [11]. It has been proposed that the first factor which influences the competition among the reaction mechanisms, by determining the adsorption mode of the reactant alcohol, is the n_B/n_A ratio, which measures whether the acid and basic functions are balanced or imbalanced in terms of number of sites. The n_B/n_A values for the present samples, reported in Table 2, clearly show the development of a basic character as the lanthanum content increases along the series. However, the information contained in the n_B/n_A ratio is not complete as it only takes into account the total concentration of the sites, whatever their strength. To better describe the acid–base properties and their influence on the catalytic behaviour, the strength of the sites is to be considered. For this purpose, the fraction of ‘strong’ sites, i.e. those with $Q_{\text{diff}}\geq 70$ kJ mol⁻¹, can be calculated. Such values ($n_{A\geq 70}/n_A$ and $n_{B\geq 70}/n_B$), also reported in Table 2, indicate that the basic sites are on average stronger than the acid ones (as can be easily observed also in Fig. 1, where the CO₂ adsorption curves lie above the NH₃ ones). In Ce75La25H, Ce50La50H and La100H, more than 3/4 of the basic sites show $Q_{\text{diff}}\geq 70$ kJ mol⁻¹, while a quite smaller fraction (zero for La100H) of acid sites exceed that limit. Although the basic sites are stronger than the acid ones also in Ce100H and Ce25La75H, the difference between the fraction of strong basic sites and the fraction of strong acid sites for these samples is sensibly lower (due to the presence of a family of acid sites with $Q_{\text{diff}}\approx 70$ –80 kJ mol⁻¹ on their surfaces).

In a forthcoming paper the catalytic behaviour of the present ceria–lanthana samples in the 4-methylpentan-2-ol conversion will be investigated and correlated with Table 2 data.

Conclusions

Adsorption microcalorimetry of suitable probe molecules (NH₃ and CO₂) provided information about the acid–base features of the ceria–lanthana system under study. Both the total concentration and the strength distribution of the sites were assessed. Development of a basic character along the series was observed. The presence of

families of basic sites of similar strength, associated with c.u.s. oxygen ions bonded to La, was revealed by steps in the Q_{diff} curves for CO₂ adsorption. The existence in the Ce₂₅La₇₅H sample of a family of acid sites similar to that of Ce₁₀₀H was tentatively ascribed to a ceria-rich phase segregated on its surface. Comparison of the present samples and another ceria-lanthana catalytic system prepared in the absence of H₂O₂ revealed some noteworthy differences, especially between La₁₀₀H and La₁₀₀ samples. Though each of them is the most basic of its series, such a basic character is expressed mainly by the very high strength of the sites for La₁₀₀ and by the unusually very high number of sites for La₁₀₀H.

The present results will form the basis for the interpretation of the catalytic behaviour of these samples, which will be dealt with in a forthcoming paper.

References

- 1 A. Auroux, in *Les techniques physiques d'étude des catalyseurs*, Eds B. Imelik and J. C. Vadrine, Ed. Technip, Institut de Recherches sur la Catalyse, 1988, p. 823.
- 2 M. Araki, K. Takahashi and T. Hibi, (Sumitomo Chemical Co.), *Eur. Pat. Appl.*, 0 150 832, 1985.
- 3 M. Araki and T. Hibi, (Sumitomo Chemical Co.), *Eur. Pat. Appl.*, 0 222 356, 1986.
- 4 A. Auroux, P. Artizzu, I. Ferino, V. Solinas, G. Leofanti, M. Padovan, G. Messina and R. Mansani, *J. Chem. Soc. Faraday Trans.*, 91 (1995) 3263.
- 5 A. Auroux, P. Artizzu, I. Ferino, R. Monaci, E. Rombi, V. Solinas and G. Petrini, *J. Chem. Soc. Faraday Trans.*, 92 (1996) 2619.
- 6 M. G. Cutrufello, I. Ferino, V. Solinas, A. Primavera, A. Trovarelli, A. Auroux and C. Picciau, *Phys. Chem. Chem. Phys.*, 1 (1999) 3369.
- 7 I. Ferino, M. F. Casula, A. Corrias, M. G. Cutrufello, R. Monaci and G. Paschina, *Phys. Chem. Chem. Phys.*, 2 (2000) 1847.
- 8 M. G. Cutrufello, I. Ferino, R. Monaci, E. Rombi and V. Solinas, *Stud. Surf. Sci. Catal.*, 140 (2001) 175.
- 9 G. Colón, J. A. Navío, R. Monaci and I. Ferino, *Phys. Chem. Chem. Phys.*, 2 (2000) 4453.
- 10 M. G. Cutrufello, I. Ferino, R. Monaci, E. Rombi, G. Colón and J. A. Navío, *Phys. Chem. Chem. Phys.*, 3 (2001) 2928.
- 11 M. G. Cutrufello, I. Ferino, R. Monaci, E. Rombi and V. Solinas, *Top. Catal.*, 19 (2002) 225.